Methods 63 (2013) 219–224

Contents lists available at SciVerse ScienceDirect

Methods

journal homepage: www.elsevier.com/locate/ymeth

# Highly sensitive and flexible inkjet printed SERS sensors on paper

Eric P. Hoppmann [a], Wei W. Yu [a], Ian M. White [b,*]

[a] 2340 Jeong H. Kim Engineering Bldg., Fischell Department of Bioengineering, University of Maryland, College Park, MD 20742, USA
[b] 2216 Jeong H. Kim Engineering Bldg., Fischell Department of Bioengineering, University of Maryland, College Park, MD 20742, USA

ARTICLE INFO

*Article history:*
Available online 17 July 2013

*Keywords:*
SERS
Sensing
Pesticides
Fungicides
Lateral flow

ABSTRACT

Surface enhanced Raman spectroscopy (SERS) has the potential to be utilized for the detection of a broad range of chemicals in trace quantities. However, because of the cost and complexity of SERS devices, the technology has been unable to fill the needs of many practical applications, in particular the need for rapid, portable, on-site detection in the field. In this work, we review a new methodology for trace chemical detection using inkjet-printed SERS substrates on paper. The detection performance of the inkjet-printed SERS devices is demonstrated by detecting 1,2-Bis(4-pyridyl)ethylene (BPE) at a concentration as low as 1.8 ppb. We then illustrate the primary advantages of paper SERS substrates as compared to conventional SERS substrates. By leveraging lateral flow concentration, the detection limit of paper SERS substrates can be further improved. Two real-world applications are demonstrated. First, the inkjet-printed SERS substrates are used as "dipsticks" for detecting the fungicide malachite green in water. Then, the flexible paper-based SERS devices are used as swabs to collect and detect trace residues of the fungicide thiram from a surface. We predict that the combination of ultra-low-cost fabrication with the advantages of easy-to-use dipsticks and swabs and the option of lateral flow concentration position ink-jet printed SERS substrates as a technology which will enable the application of SERS in solving critical problems for chemical detection in the field.



## 1. Introduction

Today there is significant interest in the development of portable and highly sensitive chemical analysis techniques for use in the field at the point of sample acquisition. Surface enhanced Raman spectroscopy (SERS) has been intensively studied for applications in chemical detection. SERS offers sensitivity comparable to that of fluorescence spectroscopy [1] while also providing highly specific information about the analyte. In Raman spectroscopy, photons from a laser source are inelastically scattered at frequencies related to the vibrational energies within the analyte molecule, and thus the measured spectrum uniquely identifies the analyte molecule. Although Raman scattering alone is a weak effect, SERS utilizes optical and chemical enhancements from gold or silver nanostructures to provide a tremendous boost to the Raman signal [2–7]. A driving force behind SERS research has been the sum of reports from over a decade ago showing that SERS enables single molecule identification [1,8–10].

Today, the most common method for performing SERS measurements is to deposit a droplet of a liquid sample onto a rigid silicon or glass substrate that has a nanostructured noble metal surface. When the sample dries, analyte molecules within the sample adsorb onto the nanostructured metal surface, where they will experience the plasmonic and chemical enhancement associated with SERS. These SERS-active surfaces can be fabricated through a number of possible techniques, including self assembly [11–14], directed or templated assembly [15–18], thin film growth [19], and nanolithography [20–22]. While nanolithography approaches tend to have high SERS enhancement factors and superior uniformity, they are complex and expensive to produce. Growth and assembly approaches are less expensive, but they suffer from problems of low throughput. Hence the techniques mentioned above are not optimized to meet the needs of widespread, routine detection of chemical species in the field.

Recently, we reported the fabrication of SERS substrates by inkjet printing silver nanostructures onto paper using a low-cost commercially available desktop piezo-based inkjet printer [23]. Other groups have reported the fabrication of SERS devices on paper and other flexible substrates through soaking [24,25] and screen printing [26]. The SERS substrates on cellulose paper demonstrate an enhancement factor of about $10^5$–$10^7$, which is on par with many of the self assembly and directed assembly techniques. In addition, the paper SERS devices have a number of advantages over rigid SERS substrates. First, liquid samples can be quickly loaded into the paper SERS device by capillary forces (wicking) simply by dipping the paper into the sample. Second, powders and

* Corresponding author.
*E-mail addresses:* hoppmann@umd.edu (E.P. Hoppmann), weiwyu@umd.edu (W.W. Yu), ianwhite@umd.edu (I.M. White).

1046-2023/$ - see front matter © 2013 Elsevier Inc. All rights reserved.
http://dx.doi.org/10.1016/j.ymeth.2013.07.010

residues, which are incredibly difficult to detect with rigid substrates or microfluidic devices, can be loaded into the paper SERS device by swabbing the inherently flexible device across a wide-area surface of any topology. Finally, analytes loaded into the paper device through dipping or swabbing can be concentrated into a small SERS sensing region by leveraging the concept of lateral flow paper fluidics. Thus, when combining the low fabrication cost of inkjet printed SERS substrates with the fluid handling properties and ease-of-use of paper-based analytics, this new paradigm represents a significant advancement in on-site analytics, and enables SERS to be much more accessible in terms of cost and usability.

In this work, we illustrate in detail the methods for fabricating paper-based SERS devices and utilizing them for applications in chemical detection. After detailing the methods for utilizing a commercial inkjet printer for fabrication, SERS spectra are presented for a range of molecules on these ink-jet printed substrates. Detection of the common model analyte 1,2-Bis(4-pyridyl)ethylene (BPE) is demonstrated at a concentration as low as 1.8 ppb. The advantage of utilizing the lateral flow concentration capabilities of the paper device are then quantified. Finally, we demonstrate two high-impact applications of the paper SERS devices. First, trace quantities of the fungicide malachite green in water are detected when the sample is loaded simply by dipping the paper SERS device into the water. Second, trace residues of the fungicide thiram are detected by swabbing a surface with a paper SERS device. This collection of results provides an in-depth view of this new low-cost and easy-to-use method for on-site analytical chemistry.

## 2. Materials and methods

### 2.1. Inkjet printed SERS substrates

Chromatography paper (0.19 mm thickness) was purchased from Fisher Scientific. Nitrocellulose membranes were purchased from Bio-Rad Laboratories (Hercules, CA). Chloroauric acid was obtained from Alfa Aesar (Ward Hill, MA). Sodium citrate and glycerol were obtained from Sigma–Aldrich (St. Louis, MO). Common commercial reagents were of analytical reagent grade.

The gold colloid is synthesized according to the method of Lee and Meisel [27]. Briefly, 80 mg of chloroauric acid is added to 400 mL of DI water (18.2 MΩ) and brought to boil in an Erlenmeyer flask. While stirring rapidly, 80 mg of sodium citrate is added. The color shifts rapidly to a deep purple. The solution is allowed to boil for 20 min and then removed from heat.

The gold ink is formed by first centrifuging the gold colloid at 6000g to concentrate the nanoparticles. After removing the supernatant the pellet of nanoparticles is suspended in water to achieve a final concentration factor of 100×. Finally, the ink is created by adding glycerol and ethanol to the concentrated nanoparticles, with a final volume ratio of 5:4:1 of concentrated nanoparticles to glycerol to ethanol. In separate work we have reported the use of silver nanoparticle ink as well [23,28].

For printing, the ink is injected into the main reservoir of refillable printing cartridges which have never contained pigmented ink. The open source vector graphics editor, Inkscape, is used to define the SERS-active regions for the printed substrates. An inexpensive consumer piezo-based inkjet printer, the EPSON Workforce 30, is used to print the SERS-active substrates onto untreated chromatography paper, as previously described [23]. Substrates are printed four times to increase the nanoparticle concentration in the paper. The flexibility of ink-jet printing allows arrays of SERS-active regions to be printed in any shape. Fig. 1A shows an array of triangular sensors printed for use in dipsticks. After printing the array, devices are cut from the paper to the appropriate size. Various paper SERS devices are displayed in Fig. 1B–D.

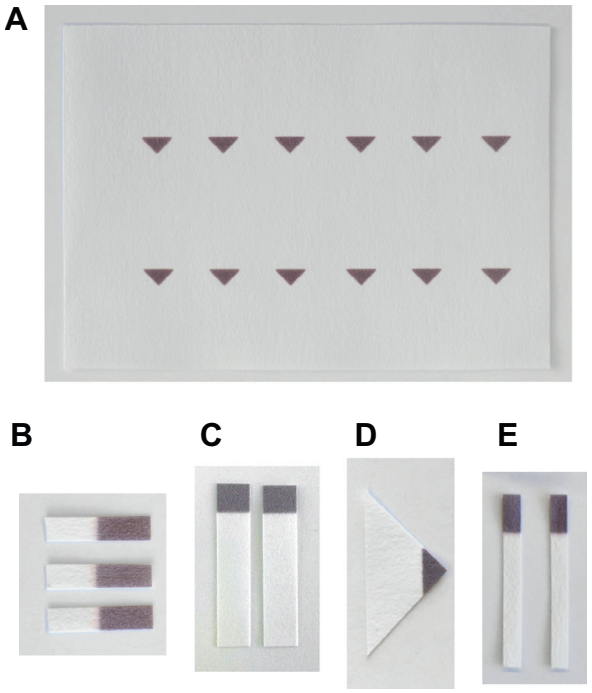


**Fig. 1.** (A) A printed array of SERS substrates. Printed arrays of SERS substrates can be cut as demanded by the application, with the goal to create a conformation that most benefits analyte collection, concentration, and detection. (B) Inkjet-printed gold nanoparticles for use as a general SERS substrate. (C) Substrates for use in lateral flow concentration experiments. (D) A substrate with a large wicking region for use as a dipstick. (E) Substrates used as surface swabs.

A scanning electron microscope (SEM) image of a typical ink-jet printed gold substrate is presented in Fig. 2, showing the clustering of gold nanoparticles in the paper fiber pores. This clustering of nanoparticles is responsible for the high SERS activity of the substrates. While the random aggregation of nanoparticles seen in Fig. 2 results in local variability of the SERS signal, the large number of nanoparticle clusters captured within the focused region of the fiber optic probe (~100 μm diameter spot) allows averaging over a multitude of nanoparticle aggregates, lowering variability and enabling quantitative results.

### 2.2. Analyte preparation

1,2-Bis(4-pyridyl)ethylene (BPE), malachite green oxalate, and thiram were obtained from Sigma–Aldrich (St. Louis, MO). BPE, malachite green, and thiram were dissolved in ethanol, water, and acetone, respectively; all samples were diluted with water to various concentrations for use as test samples.

### 2.3. SERS measurements

SERS measurements were performed using a 785 nm laser (17 mW) for excitation, a QE65000 (Ocean Optics) portable spectrometer for detection, and a fiber optic probe (InPhotonics) for delivery of laser light and collection of scattered photons (Fig. 3). The 785 nm wavelength was chosen due to the low cost and portability of 785 nm laser diodes, as well as the reduction in background fluorescence gained by operating at long wavelengths. An integration time of one second was used for all measurements; signals represent the average of three measurements. This averaging step reduces the random background noise contributed by the detector; we found that averaging across three signals was sufficient to reduce a large fraction of the noise without contributing

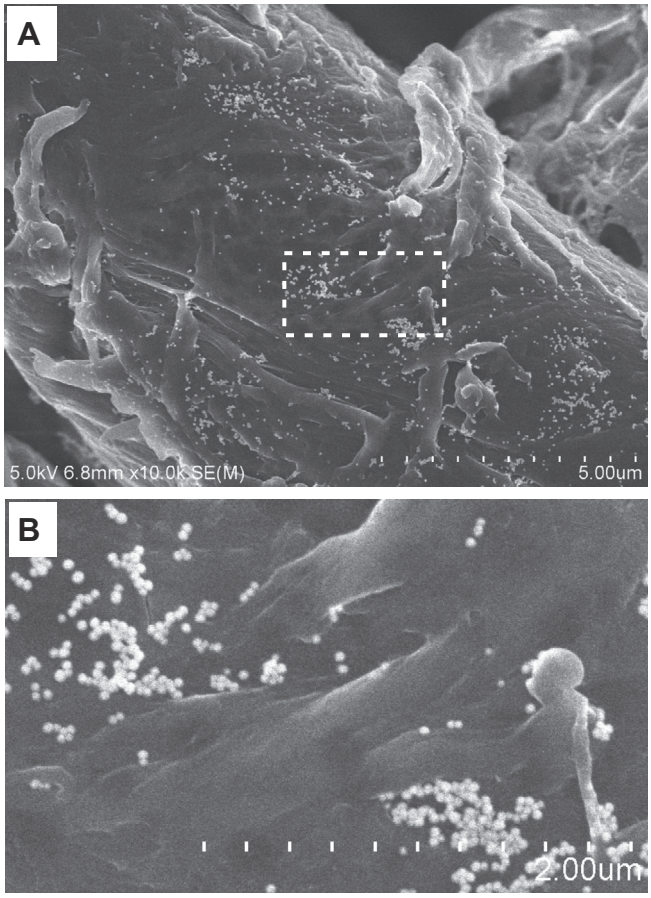


**Fig. 2.** (A) Scanning electron micrograph of a printed gold nanoparticle region on cellulose paper. (B) Clustered gold nanoparticles on the cellulose fiber (from box in (A)).

a significant amount of acquisition time. Using a linear translation stage the fiber probe was focused to maximize signal intensity for each sample before data acquisition.

For each measurement, the spectrometer records a spectrum in which the Raman scattered photons are represented by spectral peaks; the collection of peaks are used to identify the analyte. To quantify and analyze these results for sensing purposes, the following steps are taken. The magnitude (in photon counts) of the most prominent peak in the spectrum (e.g., 1207 $cm^{-1}$ for BPE) is determined by taking the difference between the value at the peak and the value at the nearest local minimum. This spectral "peak height" is considered as the signal intensity. To determine the detection limit for BPE, the signal intensity is plotted against concentration and a linear fit of the 3 lowest concentration data points is performed; the concentration at which this fit is equal to 3 standard deviations of the mean intensity (1207 $cm^{-1}$) of the blank samples is considered to be the detection limit.

In order to obtain reference spectra of the three analytes malachite green, thiram, and BPE, 2 μL droplets of each were applied to 4 × 8 mm sections of printed gold substrates (Fig. 1B, total device size 4 × 15 mm). Substrates were then dried in ambient conditions for 20 min and SERS measurements were taken as above. Each substrate was interrogated at six or more locations uniformly spread across the entire SERS active region; these spectra were averaged before plotting. SERS data from typical devices have relative standard deviations, $|\sigma/\mu|$, that range from 15% at low analyte concentrations to 5% at high analyte concentration. Cellulose paper and nitrocellulose membranes were both utilized to demonstrate the concept.

### 2.4. Lateral flow concentration

For the lateral flow concentration experiments, 30 μL of 10 ppb BPE was applied uniformly to the entire 25 × 5 mm paper strip (Fig. 1C); this volume had been pre-determined to saturate the paper strip. After drying for 20 min in ambient conditions, baseline SERS measurements were taken across the 4 × 5 mm gold region at the top of the paper strip. The bare paper end (no gold) of the dipstick was then dipped into methanol for 2 min, allowing the loaded sample to concentrate in the gold region at the top of the paper strip. Methanol was selected as the mobile phase for its high vapor pressure (faster concentration) and for the high solubility of BPE in the solvent. After the paper strip dried, the SERS signal was measured.

### 2.5. Dipsticks

An isosceles triangle with a 4 mm high SERS active region at one tip was used as a dipstick (Fig. 1D, 28 mm base and two 20 mm sides). The gold-printed region of the dipstick was dipped into a vial containing the sample of interest (in water), allowing the dipsticks to soak up liquid for either 1 or 30 s. After drying, the SERS signal was measured at 9 points forming a grid across the SERS-active region and averaged. Averaging across a relatively large number of points is necessary for two reasons: (i) SERS is infamous for signal variability when nanoparticle aggregates are used, and (ii) the analyte molecules are not uniformly distributed throughout the sensing region, a result of the location dependent rate of sample collection and concentration. This averaging methodology enables a representative picture of analyte collection and concentration even with these high-variability factors (0.33 coefficient of variation).

### 2.6. Swabs

For the swab experiments, strips of paper with 4 × 8 mm SERS-active regions at one end were used (Fig. 1E). The paper was folded

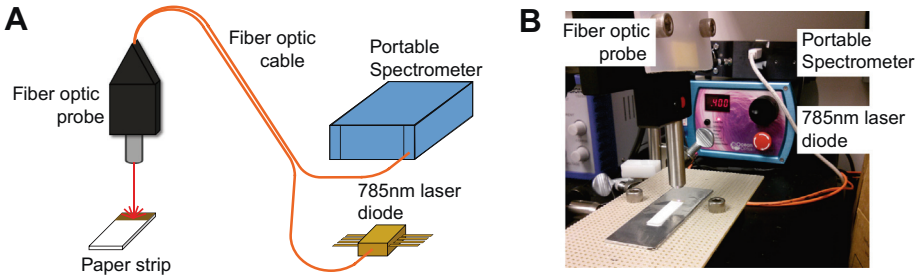


**Fig. 3.** (A) Schematic of SERS detection using a small and portable spectroscopic setup. A fiber optic probe is used for delivery of laser light and collection of scattered photons, which are delivered to a portable spectrometer. (B) Photograph of actual setup.

90 degrees where the gold region ends, and the bare end (no gold) was used to hold the swab while wiping the SERS-active region across the surface. The analyte (thiram in acetone) was applied to a clean glass slide with an approximate surface density of 1.25 ng/mm$^2$. After allowing the slide to dry, the entire swab was dipped in acetone and then carefully wiped across the entire sample-containing region of the slide twice. After drying, SERS measurements were taken across the entire SERS-active region ($n = 9$ in 3 $\times$ 3 grid) and averaged to reduce variability due to uneven sample collection. A background spectrum from an unused SERS substrate was recorded as a reference and subtracted from the recorded data.

## 3. Results and discussion

### 3.1. Identification of chemicals with paper SERS

To demonstrate that the SERS-active paper devices can be used for the spectroscopic identification of chemicals, sample droplets (2 μL) were deposited onto the region of the cellulose strips onto which nanoparticles has already been printed. Three model analytes were utilized: malachite green (1 ppm), thiram (240 ppm), and BPE (180 ppb). The respective spectrum for each analyte is presented in Fig. 4 (the upper black trace in each figure). The unique landscape of Raman peaks within each spectrum can be used to identify each molecule.

Results are also shown for the same three model analytes deposited on nanoparticle-functionalized nitrocellulose, rather than cellulose paper (the lower red traces in Fig. 4). The SERS-active nitrocellulose substrates yield strong Raman signals for BPE and thiram; however, for malachite green, the signal is significantly lower as compared to SERS-active cellulose paper. This collection of results indicates that in general, inkjet-printed SERS-active nitrocellulose membranes can also be used for chemical identification, but some molecules, such as malachite green, may have strong interactions with the nitrocellulose that inhibit adsorption onto the metal nanoparticles. Nevertheless, this demonstrates the viability of using alternate paper types for ink-jet printed SERS substrates, which provides an excellent avenue for additional assay optimization.

To further quantify the performance of the paper-based SERS devices, SERS measurements for BPE were repeated over a range of concentrations. The magnitude of the 1207 cm$^{-1}$ Raman peak is plotted versus BPE concentration in Fig. 5. The data points are fitted with a Langmuir isotherm with an $R^2$ of 0.99, which demonstrates the repeatability of our methodology. The Langmuir isotherm describes the chemical equilibrium of the interaction between BPE and the substrate, and is based on the assumption that there exist a fixed number of potential surface binding sites. This result implies that these paper-based SERS sensors can perform quantitative detection of chemicals. The detection of BPE is shown at the low concentration of 1.8 ppb (Fig. 5, inset). The limit of detection was calculated to be 1.1 ppb (12 femtomoles), which compares well with other substrates produced through directed and self-assembly, though it is not as at the same level as some reports that use sophisticated nanofabrication techniques [29–31].

### 3.2. Effect of number of print cycles on performance

The amount of gold nanoparticle ink deposited on the cellulose substrate has a direct effect on the detection sensitivity of the substrate, and is thus an important parameter to optimize when fabricating paper-based SERS substrates. To assess the impact of the number of print cycles, 2 μL of 1 ppm BPE (11 pmol) was deposited with a pipette onto inkjet-printed substrates fabricated

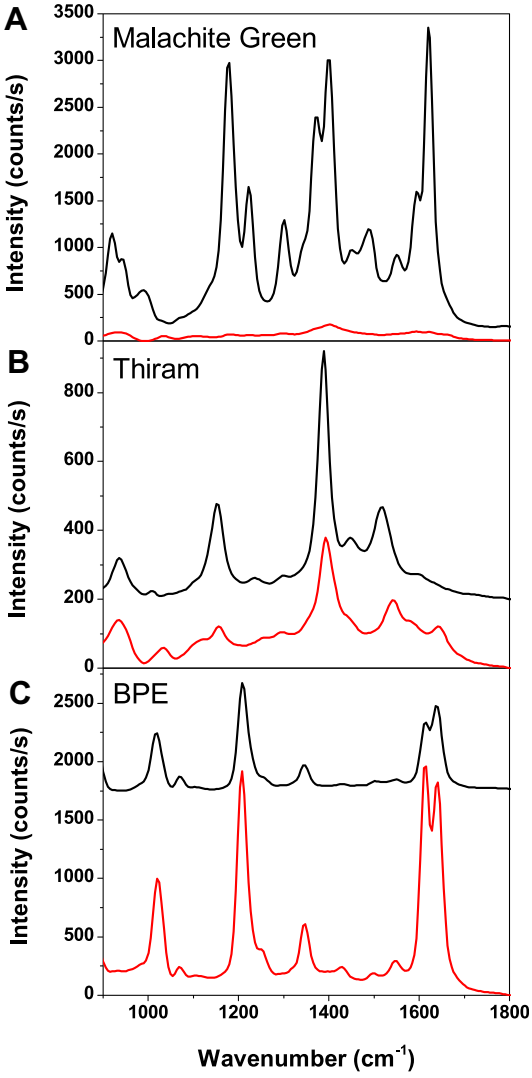


**Fig. 4.** Representative spectra of target analytes. In each figure, the top black trace is acquired using gold on cellulose substrates, while the lower red trace is acquired with gold on nitrocellulose substrates. (A) SERS signal from 2 μL of 1 ppm malachite green. (B) SERS from 2 μL of 240 ppm thiram. (C) SERS from 2 μL of 182 ppb BPE.

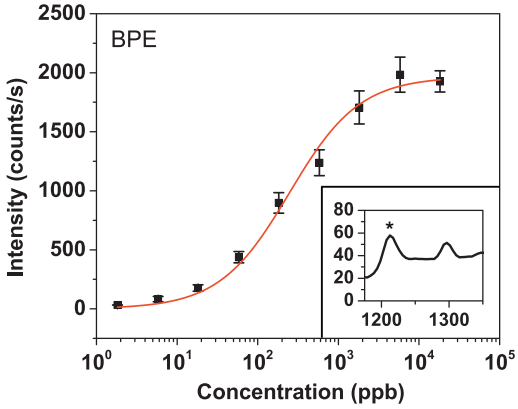


**Fig. 5.** BPE SERS signal intensity vs. concentration. Signal intensity is measured at 1207 cm$^{-1}$. Data is fitted using the Langmuir isotherm. Error bars represent the standard deviation of the 1207 cm$^{-1}$ peak height, as measured at 6 locations distributed across the SERS active region. Inset: recorded signal for 1.8 ppb BPE. Asterisk marks the 1207 cm-1 peak.

with varying numbers of print cycles. As expected, the data in Fig. 6 show a trend of increasing signal intensity with increasing print cycles, which peaks at 12 print cycles. Beyond 12 cycles, however, the measured signal begins to decline with additional print cycles. This biphasic trend appears to imply that an increasing number of nanoparticle clusters initially improves the signal, but after 12 cycles this effect is countered by interference due to excess amounts of other components in the ink. Naturally, this optimal cycle number will vary for different printers and different ink formulations.

### 3.3. Lateral flow concentration

The data in Fig. 5 demonstrates that the paper-based SERS devices can be used for the quantitative detection of trace levels of analyte in solution. Additionally, as described above, paper-based SERS devices offer a unique advantage over rigid SERS substrates; after loading a relatively large volume of liquid sample into the paper device, the analyte molecules within the paper can be concentrated into a small sensing region through lateral flow concentration. To illustrate the advantage of the lateral flow concentration step, 30 μL of BPE in water (10 ppb) was uniformly loaded into a paper strip with a pipette; Au nanoparticles had been printed at one end of the to define the sensing region. After drying the paper, the strip was dipped into methanol such that the methanol wicked into the paper and carried the analyte molecules up to the SERS-active tip of the lateral flow dipstick.

The BPE spectra before and after lateral flow concentration are presented in Fig. 7. The signal magnitude increases by nearly an order of magnitude due to the concentration of BPE molecules into the sensing region upon dipping the paper strip into the methanol mobile phase. Thus, while the inkjet-fabricated SERS substrate was shown to be highly sensitive, the inherent concentration capabilities of the paper can be leveraged to provide a significant improvement in the detection limit.

### 3.4. Application: detection of fungicide in water

Malachite green is a highly effective fungicide used in fish farms by the aquaculture industry. However, malachite green and its metabolite leucomalachite green are suspected mutagens [32], and are stored in fish tissue for extended periods of time [33]. As a result, malachite green is banned in many countries and thus its use must be monitored. To analyze a water sample for malachite green with a rigid SERS substrate, two approaches could be utilized: (i) a droplet (~2 μL) could be spotted onto the substrate and dried, or (ii) the substrate could be submerged and soaked in the water sample such that target analytes may diffuse to the substrate and possibly adsorb. In contrast, with paper-based SERS sensors, the paper strip is simply dipped into the water sample, allowing the sample to be wicked into the sensing region. This ease of use is particularly well suited for the detection of pesticides and other toxins in environmental water samples at the point of sample collection.

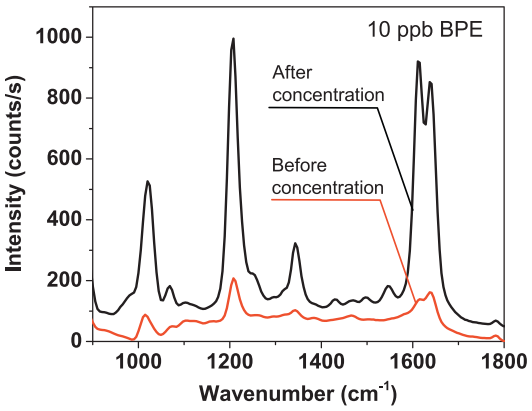


**Fig. 7.** Comparison of SERS intensity before and after lateral flow concentration.

To illustrate this application, a paper-based SERS device was dipped into malachite green (1 ppb in water). In this case, the nanoparticle-printed region of the paper strip is submerged into the sample, while the rest of the paper strip acts as a reservoir to wick in the water; as the water is drawn into the paper strip, malachite green molecules pass through the nanoparticle-printed area. The spectra recorded after a 1-s dip and a 30-s dip are shown in Fig. 8. Even after only a 1-s dip, the spectral signature of 1 ppb malachite green is clearly visible. As expected, by leaving the paper in the water sample for additional time, malachite green is continually drawn into the SERS active region, which results in an increased signal magnitude. The rate at which the analyte is drawn into the region – and thus the potential enhancement due to additional soaking time – will depend on the size of the paper reservoir. We anticipate that the paper size and dip time can be optimized based on the particular field use application and the required detection performance.

### 3.5. Application: detection of fungicide residue on a surface

Potentially the most significant advantage of paper SERS devices as compared to rigid SERS substrates may be the capability to detect residues on surfaces. One can intuit that a silicon or glass SERS device cannot be used reliably to collect trace quantities of

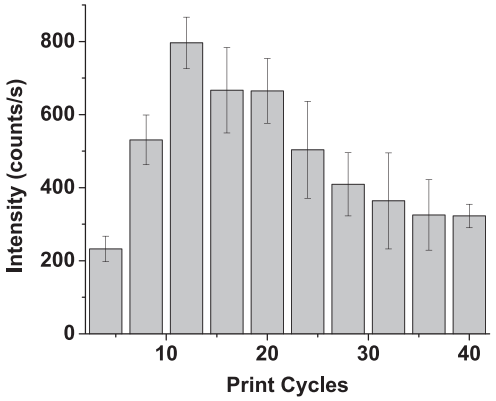


**Fig. 6.** SERS signal intensity for BPE at 1207 $cm^{-1}$ vs. number of print cycles. Error bars represent the standard deviation of the 1207 $cm^{-1}$ peak height, as measured at 6 locations distributed across the SERS active region.

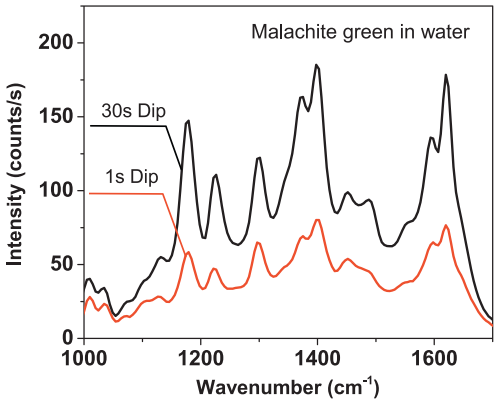


**Fig. 8.** Comparison of signal intensity for 1 and 30 s dipsticks (1 ppb malachite green in water).

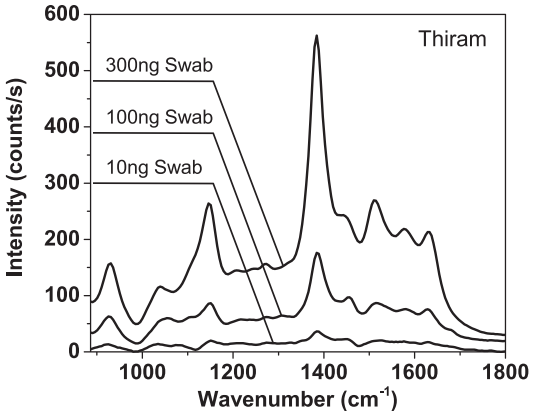


**Fig. 9.** SERS signal obtained by swabbing glass slides with various amounts of thiram deposited on the respective surfaces.

molecular residues directly from a surface, e.g., pesticide residue on a produce item. In contrast, flexible SERS substrates can be used to wipe surfaces of complex topologies. In addition, the paper can be wet such that surface-bound residues can be drawn into the paper.

To illustrate the use of paper SERS devices in this application, the fungicide thiram was deposited in known quantities onto a glass surface and allowed to dry. Then, a paper-based SERS substrate that had been wet with acetone was used to swab the surface. The Raman spectra collected for 10 ng, 100 ng, and 300 ng of thiram deposited onto the surface are shown in Fig. 9. Even with only 10 ng of fungicide present on the surface, the thiram Raman peak at 1384 $cm^{-1}$ is detectable. Thus, it is evident that paper-based SERS devices can be used to easily detect trace chemical residues directly from surfaces. This capability is expected to lead to a range of new critical applications for SERS detection in the field.

## 4. Conclusion

We have developed a new method for the fabrication of SERS substrates by inkjet printing metal nanoparticles onto paper. These devices, which are highly sensitive and yet low in cost to produce, are optimized for rapid and portable chemical detection in the field. The sensitivity of the paper SERS devices was verified by detecting BPE in concentrations as low as 1.8 ppb. In addition to low cost and high sensitivity, the paper SERS devices feature unprecedented ease of use. Two real-world applications are demonstrated to illustrate the ease of use for chemical identification at the point of sample. First, the fungicide malachite green in water (1 ppb) is detected by simply dipping the paper SERS device into the sample, causing the analyte to be wicked into the sensor. Second, residue of the fungicide thiram is detected on a surface. A clear signal is observed even when only 10 ng of the fungicide is present on the surface. Importantly, these results are achieved with a low cost portable spectrometer, further emphasizing the application of the paper SERS devices for portable on-site detection. We believe that in the near future this new method of chemical identification has great potential to fill critical needs in food safety, environmental protection, and security.

## Acknowledgment

This work was supported by the National Science Foundation, ECCS1149850. The authors acknowledge the support of the Maryland NanoCenter and its NispLab for the use of the Hitachi SU-70 Analytical UHR FEG-SEM. The NispLab is supported in part by the NSF as a MRSEC Shared Experimental Facility. In particular, the authors thank Che-Kuan Lin for assistance with obtaining the SEM images.

## References

[1] S. Nie, S. Emory, Science 275 (1997) 1102–1106.
[2] M.G. Albrecht, J.A. Creighton, J. Am. Chem. Soc. 99 (1977) 5215–5217.
[3] K. Kneipp, H. Kneipp, I. Itzkan, R.R. Dasari, M.S. Feld, Chem. Rev. 99 (1999) 2957–2976.
[4] M. Moskovits, J. Chem. Phys. 69 (1978) 4159–4161.
[5] M. Moskovits, Rev. Mod. Phys. 57 (1985) 783–826.
[6] D.L. Jeanmaire, R.P. Van Duyne, J. Electroanal. Chem. 84 (1977) 1–20.
[7] A. Campion, P. Kambhampati, Chem. Soc. Rev. 27 (1998) 241–250.
[8] K. Kneipp, H. Kneipp, V. Kartha, R. Manoharan, G. Deinum, I. Itzkan, et al., Phys. Rev. E 57 (1998) R6281–R6284.
[9] K. Kneipp, Y. Wang, H. Kneipp, L. Perelman, I. Itzkan, R. Dasari, et al., Phys. Rev. Lett. 78 (1997) 1667–1670.
[10] A.M. Michaels, M. Nirmal, L.E. Brus, J. Am. Chem. Soc. 121 (1999) 9932–9939.
[11] R.G. Freeman, K.C. Grabar, K.J. Allison, R.M. Bright, J.A. Davis, A.P. Guthrie, et al., Science 267 (1995) 1629–1632.
[12] C.J. Orendorff, A. Gole, T.K. Sau, C.J. Murphy, Anal. Chem. 77 (2005) 3261–3266.
[13] H. Wang, C.S. Levin, N.J. Halas, J. Am. Chem. Soc. 127 (2005) 14992–14993.
[14] L.M. Liz-Marza, Langmuir (2006) 32–41.
[15] D.M. Kuncicky, B.G. Prevo, O.D. Velev, J. Mater. Chem. 16 (2006) 1207.
[16] H.Y. Jung, Y.-K. Park, S. Park, S.K. Kim, Anal. Chim. Acta 602 (2007) 236–243.
[17] V. Liberman, C. Yilmaz, T.M. Bloomstein, S. Somu, Y. Echegoyen, A. Busnaina, et al., Adv. Mater. 22 (2010) 4298–4302.
[18] S. Mahajan, J. Richardson, T. Brown, P.N. Bartlett, J. Am. Chem. Soc. 130 (2008) 15589–15601.
[19] S.B. Chaney, S. Shanmukh, Appl. Phys. Lett. 87 (2005) 031908.
[20] T.R. Jensen, M.D. Malinsky, C.L. Haynes, R.P. Van Duyne, J. Phys. Chem. B 104 (2000) 10549–10556.
[21] H. Im, K.C. Bantz, N.C. Lindquist, C.L. Haynes, S.-H. Oh, Nano Lett. 10 (2010) 2231–2236.
[22] X. Deng, G.B. Braun, S. Liu, P.F. Sciortino, B. Koefer, T. Tombler, et al., Nano Lett. 10 (2010) 1780–1786.
[23] W.W. Yu, I.M. White, Anal. Chem. 82 (2010) 9626–9630.
[24] C.H. Lee, M.E. Hankus, L. Tian, P.M. Pellegrino, S. Singamaneni, Anal. Chem. 83 (2011) 8953–8958.
[25] Y.H. Ngo, D. Li, G.P. Simon, G. Garnier, J. Colloid Interface Sci. (2012) 237–246.
[26] L.-L. Qu, D.-W. Li, J.-Q. Xue, W.-L. Zhai, J.S. Fossey, Y.-T. Long, Lab Chip 12 (2012) 876–881.
[27] P.C. Lee, D. Meisel, J. Phys. Chem. 86 (1982) 3391–3395.
[28] W.W. Yu, I.M. White, Analyst 138 (2013).
[29] Karen L. Norrod, L.M. Sudnik, D. Rousell, K.L. Rowlen, Appl. Spectrosc. 51 (1997) 994–1001.
[30] W. Wu, M. Hu, F.S. Ou, Z. Li, R.S. Williams, Nanotechnology 21 (2010) 255502.
[31] Y. Liu, J. Fan, Y.-P. Zhao, S. Shanmukh, R.A. Dluhy, Appl. Phys. Lett. 89 (2006) 173134.
[32] S. Srivastava, R. Sinha, D. Roy, Aquat. Toxicol. 66 (2004) 319–329.
[33] S.J. Culp, F.A. Beland, Int. J. Toxicol. 15 (1996) 219–238.